Arabian Journal of Chemistry (2022) **15**, 103966

King Saud University

Arabian Journal of Chemistry

www.ksu.edu.sa
www.sciencedirect.com

ORIGINAL ARTICLE

5-Fluorouracil-containing inorganic iron oxide/platinum nanozymes with dual drug delivery and enzyme-like activity for the treatment of breast cancer

Zheng Nie [a], Yasaman Vahdani [b], William C. Cho [c], Samir Haj Bloukh [d,e], Zehra Edis [e,f], Setareh Haghighat [g], Mojtaba Falahati [h], Rasoul Kheradmandi [i,j], Laila Abdulmohsen Jaragh-Alhadad [k,l,*], Majid Sharifi [i,j,*]

[a] *Department of Breast Surgery, the First People's Hospital of Jingzhou, Jingzhou 434000, Hubei Province, China*
[b] *Department of Microbiology, Faculty of Pharmaceutical Science, Tehran Medical Sciences, Islamic Azad University, Tehran, Iran*
[c] *Department of Clinical Oncology, Queen Elizabeth Hospital, Kowloon, Hong Kong*
[d] *Department of Clinical Sciences, College of Pharmacy and Health Sciences, Ajman University, PO Box 346, Ajman, United Arab Emirates*
[e] *Centre of Medical and Bio-allied Health Sciences Research, Ajman University, Ajman, United Arab Emirates*
[f] *Department of Pharmaceutical Sciences, College of Pharmacy and Health Sciences, Ajman University, PO Box 346, Ajman, United Arab Emirates*
[g] *Department of Microbiology, Faculty of Advanced Science and Technology, Tehran Medical Sciences, Islamic Azad University, Tehran, Iran*
[h] *Department of Nanotechnology, Faculty of Advanced Science and Technology, Tehran Medical Sciences, Islamic Azad University, Tehran, Iran*
[i] *Student Research Committee, School of Medicine, Shahroud University of Medical Sciences, Shahroud, Iran*
[j] *Depatment of Tissue Engineering, School of Medicine, Shahroud University of Medical Sciences, Shahroud, Iran*
[k] *Department of Chemistry, College of Science, Kuwait University, Safat 13060, Kuwait*
[l] *Cardiovascular and Metabolic Sciences Department, Learner Research Institute, Cleveland Clinic, OH 44195, USA*

Received 23 September 2021; accepted 16 May 2022
Available online 20 May 2022

* Corresponding authors at: Department of Chemistry, College of Science, Kuwait University, Safat 13060, Kuwait (L.A. Jaragh-Alhadad). Student Research Committee, School of Medicine, Shahroud University of Medical Sciences, Shahroud, Iran (M. Sharifi).
E-mail addresses: Laila.alhadad@ku.edu.kw (L.A. Jaragh-Alhadad), Sharifi@shmu.ac.ir, Laila.alhadad@ku.edu.kw, Sharifi@shmu.ac.ir (M. Sharifi).

Peer review under responsibility of King Saud University.

Production and hosting by Elsevier

https://doi.org/10.1016/j.arabjc.2022.103966

KEYWORDS

Breast cancer;
5-Fluorouracil;
Nanozymes;
Fe_3O_4 nanospheres;
Cytotoxicity

Abstract Intrinsic enzyme-mimic activity of inorganic nanoparticles has been widely used for nanozymatic anticancer and antibacterial treatment. However, the relatively low peroxidase-mimic activity (PMA) and catalse-mimic activity (CMA) of nanozymes in tumor microenvironment has hampered their potential application in the cancer therapy. Therefore, in this study, we aimed to fabricate platinum (Pt) nanozymes dispersed on the surface of iron oxide (Fe_3O_4) nanosphere that, in addition to boosting the PMA and CMA, resulted in the formation of a pH-sensitive nanoplatform for drug delivery in breast cancer therapy. After development of Fe_3O_4 nanospheres containing Pt nanozymes and loading 5-fluorouracil (abbreviated as: Fe_3O_4/Pt-FLU@PEG nanospheres), the physicochemical properties of the nanospheres were examined by electron microscopy, dynamic light scattering, zeta potential, X-ray diffraction, thermogravimetric, BET surface, and PMA/CMA analyses. Then, the cytotoxicity of the Fe_3O_4/Pt-FLU@PEG nanospheres against 4T1 cells was investigated by the cell counting kit-8 assay and flow cytometry. Also, the anticancer effect of fabricated nanoplatform was assessed in mouse bearing 4T1 cancer tumors, *in vivo*. The results showed that the Fe_3O_4/Pt-FLU@PEG nanospheres provide a platform for optimal FLU loading, continuous pH-sensitive drug release, and potential PMA and CMA to increase the level of ROS and O_2, respectively. Cytotoxicity outputs showed that the Fe_3O_4/Pt-FLU@PEG nanospheres mitigate the proliferation of 4T1 cancer cells mediated by apoptosis and intracellular generation of reactive oxygen species (ROS). Furthermore, *in vivo* assays indicated a significant reduction in tumor size and overcoming tumor hypoxia. Overall, we believe that the developed nanospheres with dual enzyme-mimic activity and pH-sensitive drug delivery can be used for ROS/chemotherapy double-modality antitumor therapy.

1. Introduction

Breast cancer has the highest incident rate in women and high mortality rate, it is difficult to treat due to its low drug permeability rate and hypoxia (Semenza 2016, Zou et al. 2021). One of the non-invasive treatment strategies is the use of nanozymes with catalytic properties (Attar et al. 2019, Sharifi et al. 2020a). Nanozymes are nanomaterials with catalytic -like performances comparable to natural enzymes that have been widely used in biomedical field in recent years. They showed several unique properties including controlled catalytic activity, combination therapy, and targeted drug delivery (Falahati et al. 2022) along with higher stability, and lower cost compared to natural enzymes (Feng et al. 2022). Nanozymes can directly combat cancer cells by improving drug permeability as well as increasing intracellular reactive oxygen specious (ROS) (Skivka et al. 2018, Khan et al. 2020, Sharifi et al. 2020c). In this regard, platinum (Pt) is known as one of the important nanozymes due to both peroxidase-mimic activity (PMA) and catalse-mimic activity (CMA)(Khan et al. 2021a, Tsai et al. 2021). On the other hand, the use of Pt as a drug such as cisplatin has been reported to be effective in treating a variety of cancers (Prylutska et al., 2019a, 2019b, Rottenberg et al. 2021, Shueng et al. 2021). Although several studies have shown that iron oxide (Fe_3O_4) nanosphere has potential peroxidase-mimic performance, their limited ability against generation of free radicals and improving drug permeability can be improved by their integration with Pt. For example, report of Ma et al. (2020) shows that Pt nanozymes on the platform of porous nanospheres such as Fe_3O_4 not only effectively perform PMA, but also reduce the tendency of Pt to absorb CO/CO_2, which prevents the formation of ROS. By loading Pt on the Fe_3O_4 platform, Li et al. (2019) designed a PtFe@Fe_3O_4 nanozymes with PMA in the tumor environment, which not only combat tumor cells through increasing the intracellular ROS mediated by degrading hydrogen peroxide (H_2O_2) to radicals, but also by overcoming hypoxia enhanced the anticancer performance of the nanospheres. In addition, they showed that Fe_3O_4 nanospheres acts as an electron pump to keep Pt in an electron-rich state to stimulate both PMA and CMA. Although ceria, copper, vanadium, cobalt, and manganese nanozymes are highly suitable for their catalytic activity, Fe_3O_4 nanoparticles are widely used in biomedical studies due to their high biocompatibility and readable integration with other nanozymes (Liu et al. 2021b). On the other hand, the concurrent oxidase and peroxidase performance of PtFe@Fe_3O_4 nanozymes makes them potential platforms in the treatment of cancers (Khan et al. 2021c). Furthermore, the use of porous Fe_3O_4 platform can provide the possibility of photothermal and photodynamic therapies, which can be found in the studies of Sharifi et al. (2020b), Sharifi et al. (2020d) and Zhao et al. (2021).

5-Fluorouracil (FLU), an uracil nucleotide containing hydrogen in the fluorine atom (Baasner and Klauke 1989), is one of the most widely used compounds in the treatment of solid tumors of the gastrointestinal tract such as colorectal (Moutabian et al. 2022), pancreas (Chen et al. 2022), and liver (AlQahtani et al. 2021). This anti-metabolite compound can inhibit DNA synthesis and prevent tumor cell proliferation. Although the use of doxorubicin, paclitaxel and methotrexate drugs are show a great potential in the treatment of breast cancer, the results of Tang et al. (2022), Zheng et al. (2022), and Katharotiya et al. (2021) showed that FLU has a potential performance in the treatment of breast cancer. One of the major challenges of FLU is cytotoxicity in off-target tissues at high doses and very short half-life due to failure to cross the plasma membrane (Noguchi et al. 2021). In recent years, the use of nanocarriers to increase drug stability, reduce off-toxicity especially in cardiac tissue and improve cellular uptake in solid tumors has revived a great deal of interest in nanomedicine (Borowik et al. 2018, Hurmach et al. 2020, Afzal et al. 2021, Liu et al. 2021a, Pooresmaeil et al. 2021b). In this regard, Pooresmaeil et al. (2021a) after designing a metal–organic- framework based on chitosan-coated zinc oxide containing FLU immobilized on graphene oxide (FLU@CS/Zn-MOF@GO), revealed that not only the developed platform results in a pH-sensitive sustained drug release, but also

significantly reduces the survival rate of breast cancer cells by up to 45% compared to the free drug. Meanwhile, FLU@CS/Zn-MOF@GO also had higher biocompatibility compared to free drug. It was also shown that FLU in tamoxifen-resistant MCF-7 tumor cells not only reduced the drug resistance of cancer cells to tamoxifen, but also improved the success of breast cancer therapy by enhancing apoptosis and reducing tumor volume (Watanabe et al. 2021).

In this study, an attempt was made to design an iron oxide/Pt-fluor ouracil@polyethylene glycol (Fe_3O_4/Pt-FLU@PEG) nanospheres with dual drug delivery and PMA/CMA for the treatment of solid breast cancer tumors. In this regard, nanospheres were first produced by hydrothermal method. Although hydrothermal synthesis is relatively expensive, time consuming, and requires toxic solvents, it is wildly used as a most common methods for synthesis of nanomaterial due to several advantages including wide temperature range, feasible control of material morphology, synthesis of nanospheres with high stability, and simple integration with other production methods. After producing the nanospheres, this study considers the physicochemical properties of Fe_3O_4/Pt-FLU@PEG nanospheres and their capabilities for FLU release in acidic environment, toxicity against 4T1 cancer cells, reduction of breast tumor size, and increase of O_2 level in cancerous tissue. Because chemotherapy-based breast cancer therapy is always limited with drug resistance, lack of potential uptake of drugs and insufficient drug loading in breast tumors; we believe that the use of Fe_3O_4/Pt-FLU@PEG nanospheres with high catalytic performance can provide a great therapeutic hope for the treatment of solid breast tumors.

2. Material and methods

2.1. Materials

All chemical compounds used in the synthesis of Fe_3O_4/Pt-FLU@PEG nanospheres were purchased from Sigma Aldrich.

2.2. Synthesis of nanocarriers

2.2.1. Synthesis of Fe_3O_4 nanosphere

Fe_3O_4 nanospheres were prepared by hydrothermal method according to the report of Sharifi et al. (2020b) (Fig. 1).

2.2.2. Synthesis of Fe_3O_4/Pt-FLU@PEG

H_2PtCl_6 (200 mg), PEG 300 (100 mg) and Fe_3O_4 nanosphere samples (1 g) were dissolved in ethylene glycol solution and the solution was heated at 170 °C for 20 min in order to load the Pt nanozymes. Then, the solution was cooled and shaken vigorously at 21 °C for 7 h. Samples were collected and washed with deionized water. To load FLU, 10 mg of the nanosphere was injected into 25 mL of dimethyl sulfoxide solution containing 10 mg of FLU and kept for 24 h with a gentle shaking. The samples were then dried at room temperature for 24 h and finally washed by PBS for further assays.

2.3. Characterization of Fe_3O_4/Pt-FLU@PEG nanospheres

Scanning electron microscopy (SEM; JEOL-6700, Japan) was used to examine the surface morphology of nanospheres. Also, a high-resolution transmission electron microscope (TEM; HRTEM, JEM-2010) with an acceleration voltage of 100 kV was used. Zetasizer system (Malvern Instruments, UK) was employed to investigate the hydrodynamic size and zeta potential of nanospheres. The samples were dispersed to measure particle size in deionized water at 25 °C and examined at a dispersion angle of 90°. Also, the samples were dispersed in 0.3 mM aqueous KCl solution at a pH range of 4–9 for zeta

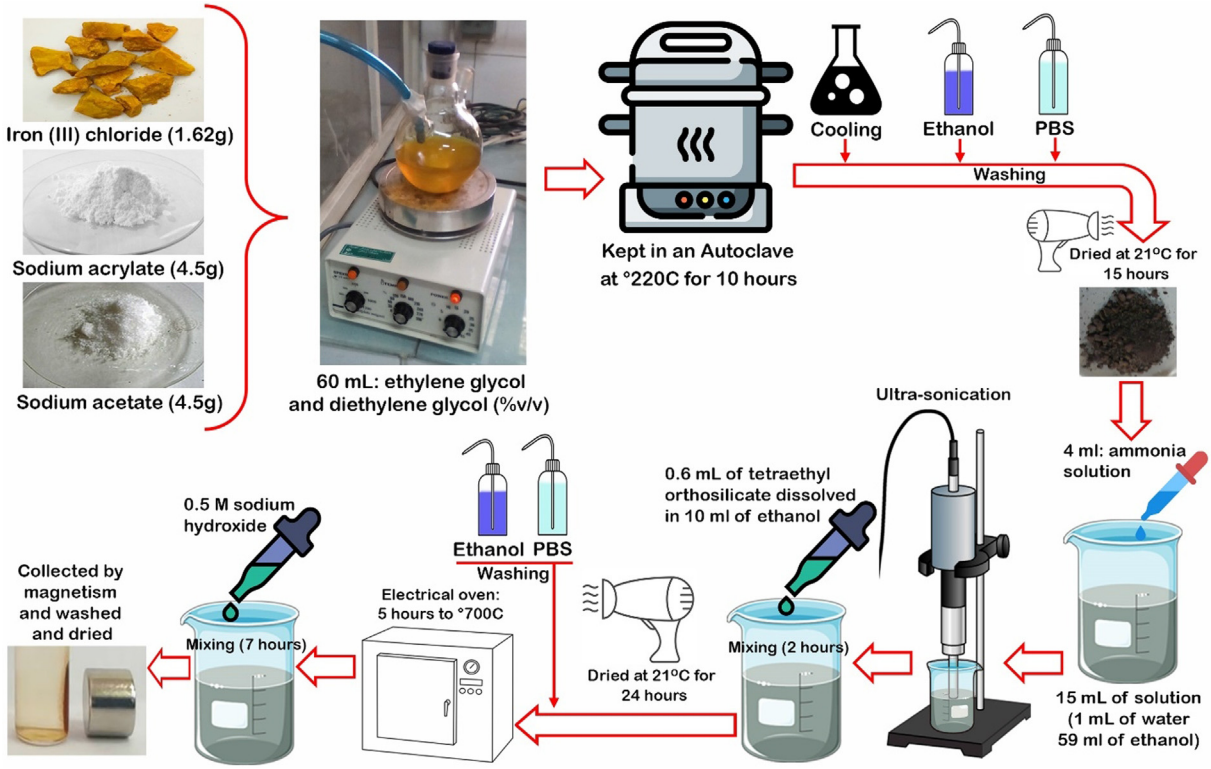

Fig. 1 Schematic view of Fe_3O_4 nanosphere synthesis.

potential measurements. In addition, atomic adsorption method based on the method of Sápi et al. (2017) was used to investigate the presence of Pt on the Fe_3O_4 nanospheres. Furthermore, to measure the nanospheres cavities, N2 adsorption isotherms at nitrogen liquid temperature (-196 °C) of Quantachrome Nova automatic gas adsorption system were applied.

XRD analysis was performed applying a D/max- with Cu Kα radiation (Rigaku, Japan) in continuous scan mode from 10–80° with a step size of 0.02° and speed of 2°/min. To investigate FTIR spectra, the samples were mixed with potassium bromide powder (KBr) and examined in the range of 500–4000 cm^{-1} with a resolution of 1 nm. In addition, the thermal stability of the Fe_3O_4/Pt nanospheres was investigated using TGA (Perkin-Elmer) under N2 with a heating rate of 5 °C/min in the range of 50–510 °C.

2.4. Drug loading and release

In order to evaluate the loading capacity and release of FLU from nanospheres, the procedures of immersion and dialysis were used, respectively. In this procedure, 200 μg of Fe_3O_4/Pt@PEG nanospheres were added to drug solutions at concentrations of 100, 200, 300, 400 and 500 μg for 24 h at room temperature with gentle shaking, followed by a magnetic-based separation. Afterwards, the remaining solution, like the initial solution, was evaluated by fluorescence spectroscopy (Hitachi F 2500 spectrophotometer). Finally, loading efficiency was measured by Eq. (1):

$$\text{Loading efficiency } (\%) = [(A - B)/B] \times 100 \quad (1)$$

where A is the total amount of FLU in initial solution and B is the amount of FLU remaining in the solution.

To evaluate the release capacity of FLU, the Fe_3O_4/Pt-FLU@PEG nanospheres at pH 6.5 and 7.4, at 37 °C for 120 min was examined using dialysis process. The amount of 100 μg Fe_3O_4/Pt-FLU@PEG nanospheres was suspended in 10 mL PBS. Then, it was put in dialysis cassettes and placed in 40 mL of the same PBS buffer with shaking at 100 rpm. At different time intervals of 6, 15, 30, 60, 90, 180, 360, 540 and 720 min, 5 mL of solution was removed for measurement by adsorption at 266 nm, where the same amount of initial buffer was added to the tank. Finally, Eq. (2) was used to evaluate the diffusion profile.

$$\text{Cumulative drug release } (\%) = \frac{5 \times \sum_{i-1}^{n-1} C_i + 50 \times C_n}{\text{weight of FLU on } Fe_3O_4/Pt - FLU@PEG} \times 100 \quad (2)$$

where C_i and C_n refer to the f FLU concentration at time i and n, respectively.

2.5. Enzyme-mimic activity assay

To investigate PMA, a UV–vis spectrometer (Shimadzu UV-2600) was used after 10 min of the Fe_3O_4, Fe_3O_4/Pt-FLU and Fe_3O_4/Pt-FLU@PEG nanospheres reaction in a solution containing hydrogen peroxide (H_2O_2) and 3,3′,5,5′-tetramethyl benzidine (TMB), based on the previous report (Chandra et al. 2019). In addition, an O_2 electrode was used in the Multi-Parameter Analyzer (JPSJ-606L, Leici China) to check the level of O_2 produced in the solution based on the catalase-mimic activity (CMA) of constructed platform, as described previously (Song et al. 2016).

2.6. In vitro studies

4T1 cancerous cells were cultured in Dulbecco's Modified Eagles Medium (DMEM) and supplemented with 10% fetal bovine serum (FBS) and 1% penicillin/streptomycin (Gibco). The flasks containing 4T1 cancerous cells were kept in the incubator with 5% CO_2, 37 °C and 95% humidity. To transfer 4T1 cancerous cells to the new culture medium, cells were trypsinized (0.25% trypsin-EDTA) and re-suspended in DMEM medium.

2.6.1. Viability of 4T1 cells

To evaluate the cytotoxicity of FLU, Fe_3O_4/Pt, and Fe_3O_4/Pt-FLU@PEG, the WST-8 (tetrazolium salt) dyeing reaction method was used by measuring the 4T1 cancerous cells proliferation via Cell Counting Kit-8 (CCK-8) (Bioworld Technology, Nanjing, China). 4×10^3 4T1 cancer cells were seeded in 96-well plates, and incubated at 37 °C with 5% CO_2. After 8 h, the cultured 4T1 cancer cells were exposed to determined concentrations of FLU (5, 15, 25, 35, and 45 μg/mL), Fe_3O_4/Pt nanospheres (10, 30, 50, 70 and 90 μg/mL), and Fe_3O_4/Pt-FLU@PEG nanospheres (10, 30, 50, 70 and 90 μg/mL). The culture medium was further incubated for 24 h. Next, the cells were washed and 100 μL of fresh medium with 15 μL CCK-8 solution (0.5 mg/mL) was added to each well. The culture medium was then incubated in the dark at 37 °C for 2 h. Finally, the optical density at 450 nm was read by a plate reader. Survival rates of treated and control cells were determined using Eq. (3).

$$\begin{aligned}\text{Cell viability } (\%) = [&[\text{Optical density of dosing cells} \\ &- \text{Optical density of blank}] \\ &\div [\text{Optical density of control} \\ &- \text{Optical density of blank}]] \times 100\end{aligned} \quad (3)$$

2.6.2. Apoptosis and ROS assays

The Annexin-V/PI Apoptosis Analysis Kit (Yeasen, Inc., China) was applied to evaluate the percentage of apoptotic cells. 4T1 cancerous cells based on Section 3.1 with a density of 3×10^5 cells/well were cultured and incubated for 12 h. Next, the cultured cells were exposed to the FLU (25 μg/mL), Fe_3O_4/Pt nanospheres (50 μg/mL), and Fe_3O_4/Pt-FLU@PEG nanospheres (50 μg/mL). The cells were then incubated at 37 °C with 5% CO_2 for 24 h. After incubation, the 4T1 cancer cells were collected by centrifugation at 1,000*g* (5 min) and washed in cold PBS.

The samples were re-suspended in 200 μL binding buffer. Afterwards, according to the manufacturer's protocol, the 4T1 cells were stained with Annexin V-FITC/Alexa Fluor 488 (5 μL) and propidium iodide (PI: 10 μL) in the dark. Finally, the data were investigated by a flow cytometer (FACSCalibur, BD Bioscience, USA). Also, to determine the level of intracellular ROS, 3×10^5 cells/well were cultured in 6-well plates, and after 8 h of incubation (5% CO_2 and 37 °C with 95% humidity) were exposed to the FLU (25 μg/mL), Fe_3O_4/Pt nanospheres (50 μg/mL), and Fe_3O_4/Pt-FLU@PEG nanospheres (50 μg/mL). The 4T1 cells further

incubated for 24 h were washed with PBS and exposed to 10 μM 2,7-dichlorodihydrofluorescein for 30 min, followed by washing with PBS. Finally, the ROS level was determined using a flow cytometer (FACSCalibur, BD Bioscience, USA) by detecting the fluorescence value of 2,7-dichlorofluorescein obtained by 2,7-dichlorodihydrofluorescein oxidation.

2.7. In vivo studies

In order to perform the treatment of breast cancer, 40 six-week-old female BALB/c mice (10 mice in each group) were prepared. Mice were fully monitored throughout the experimental period with available water and food and 12 h of darkness and 12 h of light. After culturing, 3×10^6 4T1 cancer cells were injected subcutaneously into each mouse in the left side mammary glands close to foot. Then, after 25-day, 32 mice with breast tumor were selected and treated with FLU (25 μg/100 g), Fe_3O_4/Pt nanospheres (50 μg/100 g) and Fe_3O_4/Pt-FLU@PEG nanospheres (50 μg/100 g) every 24 h by tail vein injection.

2.7.1. Tumor condition and hypoxia detection

To control abnormal behaviors, mice were monitored daily and at the end of the experimental period, the mice were sacrificed on the 25th day and the tumors were harvested and weighed by a digital scale.

Photoacoustic imaging (PA) was used to evaluate hypoxia in breast tumors. In this regard, to examine vascular saturated O_2 in tumor tissue, mice were imaged 24 h after injection. O_2-containing hemoglobin (HbO_2) and O_2-free hemoglobin (Hb) were acquired at the excitation wavelength of 850 and 700 nm, respectively, using a pre-clinical photoacoustic computed tomography scanner (Endra Nexus 128). Then, PA severity was assessed using ImageJ software (National Institutes of Health, Bethesda, USA).

2.8. Statistical analysis

The data were analyzed by one-way analysis of variance. Also, statistical significances were investigated by the Statistical Package for Social Science (SPSS: version 20) and Tukey's multiple comparison tests. P-values of < 0.05 were considered statistically significant.

3. Results and discussion

3.1. Morphology and structure properties

The morphology and size of Fe_3O_4/Pt nanospheres were determined using SEM and TEM techniques. As shown in Fig. 2A and 2B, Fe_3O_4 nanospheres have retained their morphological structure despite the deposition of Pt nanozymes on their surface. Based on the atomic adsorption results, in line with the results of Li et al. (2019) and Ma et al. (2020), it was determined that 1.8% of the Fe_3O_4/Pt nanospheres weight is composed of Pt nanozymes (data not shown). Also, Pt nanozymes can be observed on nanospheres evidenced by TEM image.

Furthermore, the TEM image represents that the size of Fe_3O_4/Pt nanospheres with FLU and PEG coating is in the range of 90–110 nm with some surface cavities. Although DLS outputs showed a hydrodynamic distribution ranging from 60 to 150 nm, the maximum size of Fe_3O_4/Pt-FLU@PEG nanospheres was found to be between 80 and 120 nm with an average of 100 ± 2.26 nm (Fig. 2C). In addition, the DLS results indicate successful loading of FLU and PEG coating, which increased the Fe_3O_4/Pt nanospheres dimensions up to 6 nm from 94 ± 3.12 nm in Fe_3O_4/Pt to an average of 100 ± 2.26 nm in Fe_3O_4/Pt-FLU@PEG nanospheres. In this regard, the results of zeta potential in different pH values in the presence of FLU and PEG indicated the successful loading of drug as well as polymer on the Fe_3O_4/Pt nanospheres (Fig. 2D). FLU and PEG covered the surface of nanosphere and adsorbed onto the particles thereby reducing negative surface charge across a wide range of pH values. In this study, it was revealed that iron nanosphere has a negative charge in all studied pH values, which is very suitable for loading of FLU and PEG containing a positive charge. However, in pH 9 and then pH 7, FLU and PEG can be potentially loaded on the surface of nanospheres by enhancing the negative surface charges. In this regard, it has been shown that by increasing the negative surface charge in pH ranging from 6 to 9, the maximum drug loading can be observed along with reducing the aggregation of nanocarriers (Akay et al. 2017). On the other hand, negative charge on the surface of the Fe_3O_4/Pt nanosphere, especially in physiological pH (7.2–7.4), could cause further stability of the nanospheres and reduce their associated aggregation in the blood, which previously reported by Poller et al. (2017). The porous structure of the Fe_3O_4/Pt nanospheres was confirmed by the nitrogen uptake and desorption output as shown in Fig. 2E and 2F. The results of N2 adsorption–desorption isotherm indicate an IV behavior with apparent residual loops in the range of 0.40–0.70 and 0.85–1.0P/P0. The surface area for Fe_3O_4 nanospheres was estimated to be 112.13 m^2/g, which was reduced to 88.93 m^2/g in the presence of Pt nanozymes with apparent residual loops in the range of 0.45–0.55 and 0.95–1.0 P/P0. This reduction can be considered as a relative change in the porous structure of Fe_3O_4/Pt nanospheres by Pt nanozymes deposition and a reduction in surface area or relative occlusion of cavities (Ma et al. 2020).

In the following, the output of the XRD pattern in Fig. 3A shows that the intense diffraction peaks of Fe_3O_4 nanospheres are located at 2θ = 19.5°, 31°, 35.5°, 37°, 44°, 54°, 56.5° and 63.5°. With the presence of Pt nanozymes, no change was observed in the peaks, but their intensity was slightly reduced. Therefore, the results show that not only hydrothermal method leads to the formation of well-defined crystal structures in Fe_3O_4/Pt nanospheres, but also based on the presence of Pt (according to the result of atomic adsorption), it can be stated that Pt nanozymes are uniformly distributed on the surface of nanospheres.

Also, the output of the FTIR spectrum (Data not shown) exhibits that the FLU and PEG are loaded on the surface of Fe_3O_4 nanospheres with the disappearance of peaks at 2850 cm^{-1} (C—H) and 800 cm^{-1} (C—F) in FLU; 2900 cm^{-1} (C—H), 1800 cm^{-1} (C—O), and 810 cm^{-1} (C—H) in PEG; and intensification of peaks at 3300 cm^{-1} (N—H), 1750 cm^{-1} (C═O), and 1350 (C—H) cm^{-1} in FLU; 3600 cm^{-1} (N—H) and 1200 cm^{-1} (C—O—C) in the PEG; 3650 cm^{-1} (N—H), 1650 cm^{-1} (C—O), and 700 cm^{-1} (C—C) in the Fe_3O_4/Pt nanospheres. Together with the results of imaging, DLS and FTIR, the TGA assay in Fig. 3B revealed that the samples had a

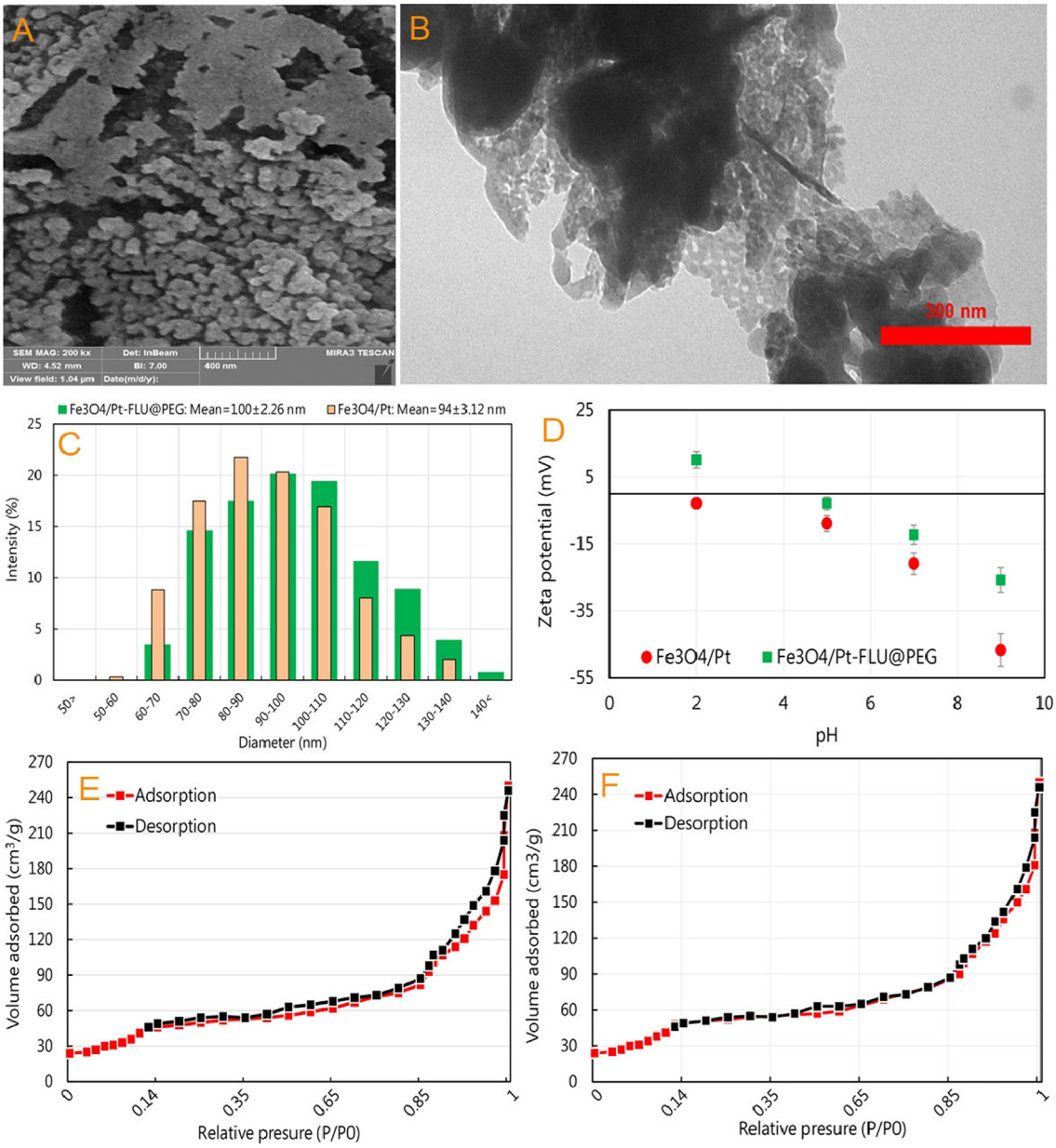

Fig. 2 (A) SEM and (B) TEM images of iron oxide/platinum-fluorouracil@polyethylene glycol (Fe_3O_4/Pt-FLU@PEG), (C) the size distribution of Fe_3O_4/Pt nanospheres and Fe_3O_4/Pt-FLU@PEG nanospheres, (D) Zeta potential values of Fe_3O_4/Pt nanospheres and Fe_3O_4/Pt-FLU@PEG nanospheres, N2 adsorption–desorption isotherms of (E) Fe_3O_4 and (F) Fe_3O_4/Pt nanospheres.

slight weight loss due to water loss at temperatures between 90 and 150 °C. With increasing temperature up to 390–400 °C, the weight loss of Fe_3O_4/Pt-FLU and Fe_3O_4/Pt-FLU@PEG seems to be due to the removal of FLU (up to 8% by weight of nanocarriers) and FLU + PEG (up to 14% by weight of nanocarriers). These results confirm the successful loading of the FLU and PEG.

3.2. Drug loading and release

As can be seen in Fig. 3C, increasing the FLU concentration dramatically increases its loading rate in the Fe_3O_4/Pt@PEG nanospheres, provided the constant concentration of the nanosphere. However, the percentage of drug loading efficiency decreased with increasing FLU concentration. Overall, the output represents the highest percentage of drug loading efficiency (more than 55%) in the range of 200 µof drug in Fe_3O_4/Pt@PEG nanospheres. This finding is in agreement with Sharifi et al. (2020d) and Benyettou et al. (2016) who indicated that the percentage of drug loading in iron oxide nanospheres with dimensions of 80–130 nm is between 47 and 60%.

The release of FLU from the Fe_3O_4/Pt-FLU@PEG nanospheres was performed at 37 °C within two different pH, 6.5 and 7.4. The output showed that FLU release in acidic medium is higher than that of in neutral medium (77.8% vs. 41.9%) and FLU release in both media has a time-dependent profile (Fig. 3D). On the other hand, the burst release of the FLU from the Fe_3O_4/Pt-FLU@PEG at pH 6.5 is 41.8% that

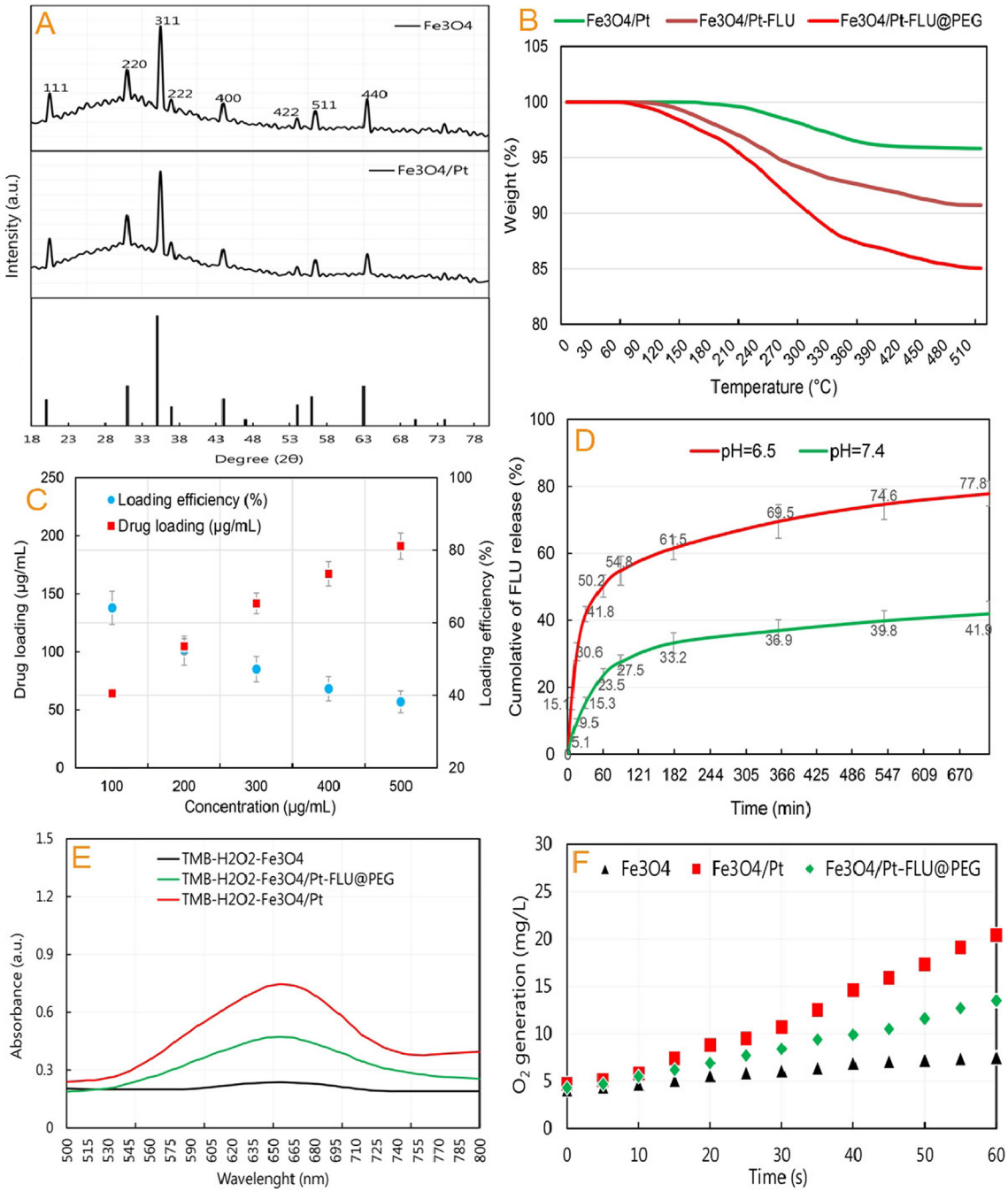

Fig. 3 (A) XRD patterns of iron oxide/platinum (Fe_3O_4/Pt) nanospheres, (B) thermogravimetric analysis of nanospheres, and the weight loss after 500 °C heating, (C) FLU loading and efficiency, (D) Quantitative analyses of FLU release at 37 °C at pH 6.5 and 7.4, (E) Peroxidase-mimic activity (PMA) of Fe_3O_4 nanospheres, Fe_3O_4/Pt nanospheres, and Fe_3O_4/Pt-FLU@PEG nanospheres, and (F) Catalase-mimic activity (CMA) of Fe_3O_4 nanospheres, Fe_3O_4/Pt nanospheres, and Fe_3O_4/Pt-FLU@PEG nanospheres.

is higher than that in the neutral medium with a rare of 15.3%. Breast cancer tumors often have a pH environment between 6 and 6.5 (Yang et al. 2017, Sharifi et al. 2021). Since Fe_3O_4/Pt-FLU@PEG nanospheres experience a pH environment of 6 to 6.5 in tumor tissue, drug release in this pH is particularly critical, which in this study based on Fig. 3, a favorable release for the FLU is conceivable. On the other hand, the FLU release behavior including burst release, velocity and process of the Fe_3O_4/Pt-FLU@PEG is strongly related to the pH of the environment (Fig. 3D), which can be considered due to increased FLU solubility (Ehi-Eromosele et al. 2017, Zorrilla-Veloz et al. 2018) and opening of PEG gates from Fe_3O_4/Pt-FLU@PEG nanospheres cavities (Khan et al. (2021b). In this study, it was found that the Fe_3O_4/Pt-FLU@PEG in each pH value has the characteristics of rapid drug release, which is saturated after one hour. This initial burst release may be related to the weak drug interaction at the Fe_3O_4/Pt surface. However, drug release from the Fe_3O_4/Pt-FLU@PEG follows first order

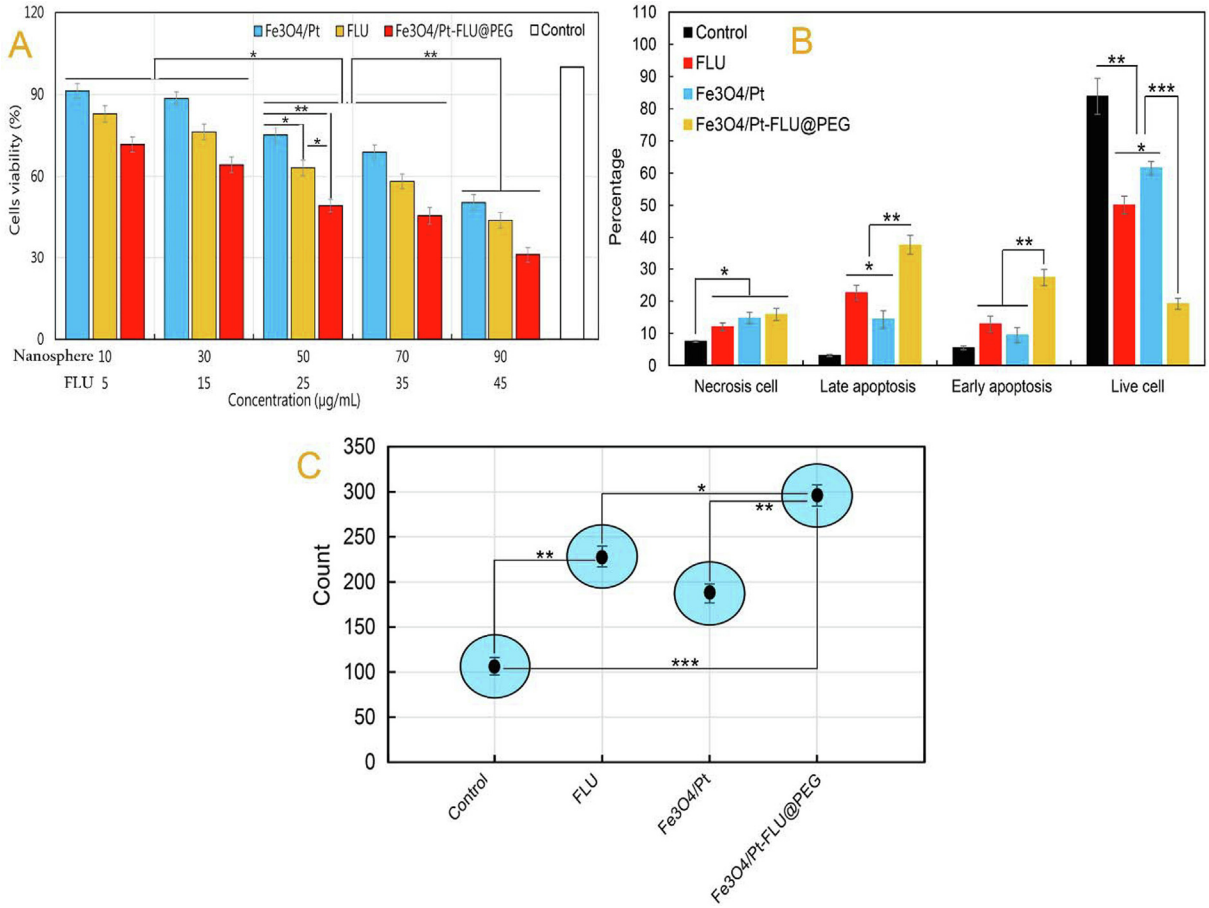

Fig. 4 (A) Cell viability of 4T1 cancerous cells incubated with iron oxide (Fe_3O_4) nanospheres, 5-Fluorouracil (FLU), iron oxide/platinum (Fe_3O_4/Pt) nanosphere, and iron oxide/platinum-fluorouracil@polyethylene glycol (Fe_3O_4/Pt-FLU@PEG) nanospheres, (B) The percentage of apoptotic cells determined by flow cytometry assay in 4T1 cells, (C) The level of ROS generation. *P < 0.05, **P < 0.01 and ***P < 0.001 for a difference of treatment groups.

release kinetics. This release index is in line with previous studies by Sharifi et al. (2020d) and Sharifi et al. (2020b), with a minor difference that the rate of drug release has slightly decreased. All in all, the release of drugs in a pH-sensitive manner is expected to result in further accumulation of FLU in tumor with higher acidity, which is a very important issue in tumor targeting and cancer nanomedicine treatment potency (Grebinyk et al. 2021, Khan et al. 2021d).

3.3. Fe_3O_4/Pt-FLU@PEG catalytic activity

Investigation of the catalytic activity of the Fe_3O_4/Pt-FLU@PEG nanospheres in the presence of H_2O_2 indicates the potential PMA of this platform. However, the output of Fig. 3E shows that FLU and PEG loading significantly reduced the PMA of the Fe_3O_4/Pt nanospheres in TMB degradation. However, the catalytic properties of the Fe_3O_4/Pt-FLU@PEG nanospheres are expected to increase with FLU release and PEG degradation in tumor tissues. In this regard, Ma et al. (2020) and Zhao et al. (2016) revealed that Pt on FeO_x platform have potential PMA in the presence of H_2O_2. Also, Li et al. (2019) showed that increasing the acidity of the environment can effectively increase the PMA of PtFe@Fe_3O_4 particles, which increases the possibility of enhancing the catalytic activity of Fe_3O_4/Pt-FLU@PEG nanospheres in tumor tissues due to PEG degradation and FLU release in acidic environments. In addition, the O_2 production output in Fig. 3F shows that the Fe_3O_4/Pt nanospheres produces higher level of O_2 (20.4 mg/L) than that of the Fe_3O_4/Pt-FLU@PEG nanospheres (13.5 mg/L). Therefore, the increase in O_2 production by Fe_3O_4/Pt-FLU@PEG nanospheres compared to that of Fe_3O_4 indicates the potential anticancer effect of the Fe_3O_4/Pt-FLU@PEG through targeting hypoxia, which is likely mediated by CMA of these platforms, altough it needs futher investigation in the future studies. According to the studies of Li et al. (2019) and Xu and Wang (2012), it can be indicated that the PMA of Fe_3O_4/Pt-FLU@PEG nanospheres cause the decomposition of H_2O_2, which may enhance the production of ROS with the possible presence of Fe^+ in Fe_3O_4/Pt-FLU@PEG nanospheres and propable CMA of these nanomaterials.

3.4. Cytotoxicity of Fe_3O_4/Pt-FLU@PEG

CCK assay and flow cytometry analysis were used to evaluate the toxicity of nanospheres and FLU on 4T1 cancerous cells. The CCK assay output in Fig. 4A shows that the toxicity of Fe_3O_4/Pt nanospheres, FLU and Fe_3O_4/Pt-FLU@PEG nano-

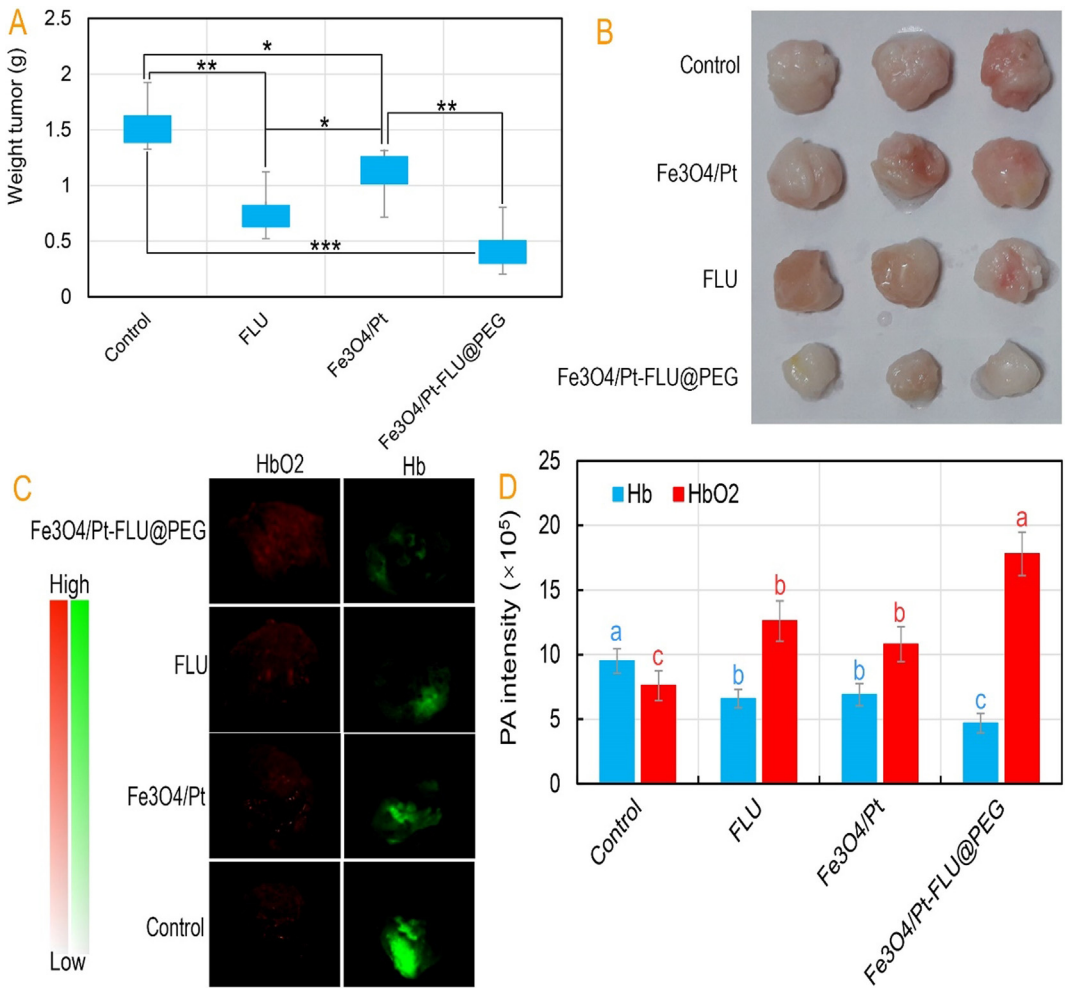

Fig. 5 (A) Tumor volume of mice in control, iron oxide (Fe_3O_4) nanospheres, 5-Fluorouracil (FLU), iron oxide/platinum (Fe_3O_4/Pt) nanosphere, and iron oxide/platinum-fluorouracil@polyethylene glycol (Fe_3O_4/Pt-FLU@PEG) nanospheres groups during 25 days of treatments and (B) its digital photographs recorded after therapy, (C) Photoacoustic (PA) images of breast tumor tissues 24 h after injection and (D) PA intensity of HbO_2 and Hb 24 h after injection. *$P < 0.05$, **$P < 0.01$ and ***$P < 0.001$ for a difference of treatment groups. [a,b,c,d]Least square means with different letters in superscripts are different at *$P < 0.05$.

spheres against 4T1 cancer cells is dose-dependent, which was in good agreement with outcomes reported by Li et al. (2019), Sharifi et al. (2020e), Liu et al. (2021a), Watanabe et al. (2021). The data in this study revealed that the highest suppression of 4T1 cancerous cells was related to the concentrations of 90 μg/ml Fe_3O_4/Pt-FLU@PEG and 45 μg/ml FLU compared to the control. Although concentrations of 70 μg/ml and 50 μg/ml Fe_3O_4/Pt-FLU@PEG compared to controls significantly reduced the growth of 4T1 cells, no significant differences were observed between them. Similarly, no differences were observed between concentrations of 10 μg/ml and 30 μg/ml in Fe_3O_4/Pt or Fe_3O_4/Pt-FLU@PEG nanospheres and between concentrations of 5 μg/ml and 7.5 μg/ml in FLU. In addition, although the use of FLU suppressed the growth of 4T1 cancer cells in a concentration-dependent manner, the use of nanocarriers significantly increased the rate of FLU cytotoxicity at all studied concentrations compared to that of the free FLU. Also, increasing the concentration of Fe_3O_4/Pt nanospheres, like other groups, further increased the rate of cytotoxicity against cancer cells. But the rate of Fe_3O_4/Pt nanospheres cytotoxicity against 4T1 cells was not significant in the initial concentration of 10 μg/mL and 30 μg/mL. Therefore, based on the results of Fig. 4A, to analyze the percentage of apoptotic cells and therapeutic activities, concentrations of 50 μg/mL Fe_3O_4/Pt-FLU@PEG nanospheres and 25 μg/mL FLU were used with a 50.7% and 36.9%, reduction in the viability of 4T1 cells, respectively (Fig. 4A). In addition, the flow cytometry output in Fig. 4B shows that 4T1 cancer cells incubated with 25 μg/mL FLU increased the induction of late apoptosis (Q2: 22.59% vs 3.12%) and early apoptosis (Q3: 12.91% vs 5.52%) compared with control sample, which was in agreement with study of Asara et al. (2013) and Gao et al. (2015). While, the use of 50 μg/mL of Fe_3O_4/Pt-FLU@PEG nanospheres containing 25 μg/mL of FLU further increased the percentage of apoptotic cells in Q2 (37.63%) and Q3 (27.32%) compared to free FLU (Fig. 4B). In agreement with our results, Arami et al. (2017) and Khan et al. (2021c) revealed that the use of nanocarriers significantly increases

the percentage of apoptotic cells, which may indicate a decrease in cancer drug resistance. In this line, ROS output, which is one of the key factors in inducing apoptosis by Fe_3O_4 and Pt (Rashid et al. 2019), shows that the use of Fe_3O_4/Pt-FLU@PEG nanospheres and FLU significantly increases the rate of ROS production. Indeed, 2.78- and 2.14-fold increase was detected in the rate of ROS generation in the Fe_3O_4/Pt-FLU@PEG nanospheres and FLU -treated groups, respectively, compared to the control (Fig. 4C). Therefore, the use of drug-containing nanocarriers can effectively suppress 4T1 cancer cells.

3.5. Tumor condition

As shown in Fig. 5A and B, Fe_3O_4/Pt nanospheres, FLU, and Fe_3O_4/Pt-FLU@PEG nanospheres could result in the potential treatment of breast cancer. After 25 days, it was determined that Fe_3O_4/Pt nanospheres, FLU, and Fe_3O_4/Pt-FLU@PEG nanospheres had a significant reduction in tumor weight compared to control. However, the results show that tumor weight loss in the Fe_3O_4/Pt-FLU@PEG nanospheres-treated group was more than 2-fold than that of the free drug and 3-fold than that of the Fe_3O_4/Pt nanosphere. This finding is in agreement with the findings of Liu et al. (2021a), Xiao et al. (2021) and Cao et al. (2021) who explained that the use of free FLU or loaded one along with Pt nanozymes effectively result in the treatment of cancer. In addition, it has been suggested that tumor size loss is directly related to increased O_2 levels due to enhanced drug permeability in solid tumors (Ikeda et al. 2016). So, in this study, hypoxia trial was performed by PA imaging to measure Hb with and without O_2 in tumor tissues.

The hypoxia test outputs in Fig. 5C and D show that the highest PA signal for HbO_2 is generated by Fe_3O_4/Pt-FLU@PEG nanospheres followed by FLU drug. Whereas, the lowest PA signal for Hb is observed in the Fe_3O_4/Pt-FLU@PEG treated group. Although the PA signal of Hb was not different between the FLU and Fe_3O_4/Pt nanospheres and even with the control, the PA signal of HbO_2 in the FLU was higher than those groups. In this regard, Chen et al. (2017), Ma et al. (2019), and You et al. (2020) recognized that the use of FLU along with Pt nanozymes increase the level of O_2 concentration and accordingly accelerate the achievement of cancer therapy. Overall, increased O_2 levels by the Fe_3O_4/Pt-FLU@PEG nanospheres along with tumor weight loss raised hopes for treatment of breast cancer through non-invasive activities.

4. Conclusions

In this study, fabricated Fe_3O_4/Pt-FLU@PEG nanospheres were shown to display both PMA and CMA for deep breast cancer therapy. After evaluating the physicochemical properties, the FLU release profile from the Fe_3O_4/Pt-FLU@PEG nanospheres indicates a stable and pH-sensitive drug release in acidic condition similar to that of tumor microenvironment. Most interestingly, the PMA and CMA of Fe_3O_4/Pt-FLU@PEG nanospheres was also revealed to increase ROS and O_2 levels, respectively. In addition, cytotoxicity assessments by CCK assay and flow cytometry showed high cytotoxicity of the Fe_3O_4/Pt-FLU@PEG nanospheres against breast cancer cells. Furthermore, *in vivo* results exhibited that the Fe_3O_4/Pt-FLU@PEG nanospheres has a great capacity to potentially overcome tumor hypoxia and reduce tumor weight. In conclusion, this study demonstrates a good prospect for the treatment of breast tumors through simultaneous drug delivery and PMA.

Ethical approval

Research experiments conducted in this article with animals were conducted as per the guidelines of the Animal Ethics Committee (AEC) of our research organization following all guidelines, regulations, legal, and ethical standards as required for animal studies.

Declaration of Competing Interest

The authors declare that they have no known competing financial interests or personal relationships that could have appeared to influence the work reported in this paper.

Acknowledgements

None.

References

Afzal, M., Ameeduzzafar, Alharbi, K.S., Alruwaili, N.K., Al-Abassi, F.A., Al-Malki, A.A.L., Kazmi, I., Kumar, V., Kamal, M.A., Nadeem, M.S., Aslam, M., Anwar, F., 2021. Nanomedicine in treatment of breast cancer – A challenge to conventional therapy. Semin. Cancer Biol. 69, 279–292.

Akay, S., Kayan, B., Yang, Y., 2017. Solubility and Chromatographic Separation of 5-Fluorouracil under Subcritical Water Conditions. J. Chem. Eng. Data 62, 1538–1543.

AlQahtani, S.A., Harisa, G.I., Alomrani, A.H., Alanazi, F.K., Badran, M.M., 2021. Improved pharmacokinetic and biodistribution of 5-fluorouracil loaded biomimetic nanoerythrocytes decorated nanocarriers for liver cancer treatment. Colloids Surf., B 197, 111380.

Arami, S., Mahdavi, M., Rashidi, M.-R., Yekta, R., Rahnamay, M., Molavi, L., Hejazi, M.-S., Samadi, N., 2017. Apoptosis induction activity and molecular docking studies of survivin siRNA carried by Fe_3O_4-PEG-LAC-chitosan-PEI nanoparticles in MCF-7 human breast cancer cells. J. Pharm. Biomed. Anal. 142, 145–154.

Asara, Y., Marchal, J.A., Carrasco, E., Boulaiz, H., Solinas, G., Bandiera, P., Garcia, M.A., Farace, C., Montella, A., Madeddu, R., 2013. Cadmium modifies the cell cycle and apoptotic profiles of human breast cancer cells treated with 5-fluorouracil. Int. J. Mol. Sci. 14, 16600–16616.

Attar, F., Shahpar, M.G., Rasti, B., Sharifi, M., Saboury, A.A., Rezayat, S.M., Falahati, M., 2019. Nanozymes with intrinsic peroxidase-like activities. J. Mol. Liq. 278, 130–144.

Baasner, B., Klauke, E., 1989. A new route to the synthesis of 5-fluorouracil. J. Fluorine Chem. 45, 417–430.

Benyettou, F., Ocadiz Flores, J.A., Ravaux, F., Rezgui, R., Jouiad, M., Nehme, S.I., Parsapur, R.K., Olsen, J.-C., Selvam, P., Trabolsi, A., 2016. Mesoporous γ-Iron Oxide Nanoparticles for Magnetically Triggered Release of Doxorubicin and Hyperthermia Treatment. Chem. – Eur. J. 22, 17020–17028.

Borowik, A., Prylutskyy, Y., Kawelski, Ł., Kyzyma, O., Bulavin, L., Ivankov, O., Cherepanov, V., Wyrzykowski, D., Kaźmierkiewicz, R., Gołuński, G., 2018. Does C60 fullerene act as a transporter of small aromatic molecules? Colloids Surf., B 164, 134–143.

Cao, H., Yang, Y., Liang, M., Ma, Y., Sun, N., Gao, X., Li, J., 2021. Pt@ polydopamine nanoparticles as nanozymes for enhanced photodynamic and photothermal therapy. Chem. Commun. 57, 255–258.

Chandra, S., Singh, V.K., Yadav, P.K., Bano, D., Kumar, V., Pandey, V.K., Talat, M., Hasan, S.H., 2019 Apr. Mustard seeds derived fluorescent carbon quantum dots and their peroxidase-like activity for colorimetric detection of H2O2 and ascorbic acid in a real sample. Analytica Chimica Acta. 25 (1054), 145–156.

Chen, J., Qiu, M., Zhang, S., Li, B., Li, D., Huang, X., Qian, Z., Zhao, J., Wang, Z., Tang, D., 2022. A calcium phosphate drug carrier loading with 5-fluorouracil achieving a synergistic effect for pancreatic cancer therapy. J. Colloid Interface Sci. 605, 263–273.

Chen, Y., Sun, L., Guo, D., Wu, Z., Chen, W., 2017. Co-delivery of hypoxia inducible factor-1α small interfering RNA and 5-fluorouracil to overcome drug resistance in gastric cancer SGC-7901 cells. J. Gene Med. 19, e2998.

Ehi-Eromosele, C., Ita, B., Iweala, E., 2017. Silica coated LSMO magnetic nanoparticles for the pH-Responsive delivery of 5-Fluorouracil anticancer drug. Colloids Surf., A 530, 164–171.

Falahati, M., Sharifi, M., Ten Hagen, T.L., 2022. Explaining chemical clues of metal organic framework-nanozyme nano-/micro-motors in targeted treatment of cancers: benchmarks and challenges. J. Nanobiotechnol. 20, 1–26.

Feng, N., Liu, Y., Dai, X., Wang, Y., Guo, Q., Li, Q., 2022. Advanced applications of cerium oxide based nanozymes in cancer. RSC Adv. 12, 1486–1493.

Gao, Y., Huo, X., Dong, L., Sun, X., Sai, H., Wei, G., Xu, Y., Zhang, Y., Wu, J., 2015. Fourier transform infrared microspectroscopy monitoring of 5-fluorouracil-induced apoptosis in SW620 colon cancer cells. Mol. Med. Rep. 11, 2585–2591.

Grebinyk, A., Prylutska, S., Grebinyk, S., Evstigneev, M., Krysiuk, I., Skaterna, T., Horak, I., Sun, Y., Drobot, L., Matyshevska, O., 2021. Antitumor efficiency of the natural alkaloid Berberine complexed with C60 fullerene in Lewis lung carcinoma in vitro and in vivo. Cancer Nanotechnol. 12, 1–18.

Hurmach, Y., Rudyk, M., Prylutska, S., Hurmach, V., Prylutskyy, Y. I., Ritter, U., Scharff, P., Skivka, L., 2020. C60 fullerene governs doxorubicin effect on metabolic profile of rat microglial cells in vitro. Mol. Pharm. 17, 3622–3632.

Ikeda, Y., Hisano, H., Nishikawa, Y., Nagasaki, Y., 2016. Targeting and treatment of tumor hypoxia by newly designed prodrug possessing high permeability in solid tumors. Mol. Pharm. 13, 2283–2289.

Katharotiya, K., Shinde, G., Katharotiya, D., Shelke, S., Patel, R., Kulkarni, D., Panzade, P., 2021. Development, evaluation and biodistribution of stealth liposomes of 5-fluorouracil for effective treatment of breast cancer. J. Liposome Res., 1–13

Khan, S., Babadaei, M.M.N., Hasan, A., Edis, Z., Attar, F., Siddique, R., Bai, Q., Sharifi, M., Falahati, M., 2021a. Enzyme–polymeric/inorganic metal oxide/hybrid nanoparticle bio-conjugates in the development of therapeutic and biosensing platforms. J. Adv. Res.

Khan, S., Hasan, A., Attar, F., Babadaei, M.M.N., Zeinabad, H.A., Salehi, M., Alizadeh, M., Hassan, M., Derakhshankhah, H., Hamblin, M.R., Bai, Q., Sharifi, M., Falahati, M., ten Hagen, T. L.M., 2021b. Diagnostic and drug release systems based on microneedle arrays in breast cancer therapy. J. Control. Release 338, 341–357.

Khan, S., Sharifi, M., Bloukh, S.H., Edis, Z., Siddique, R., Falahati, M., 2020. In vivo guiding inorganic nanozymes for biosensing and therapeutic potential in cancer, inflammation and microbial infections. Talanta, 121805.

Khan, S., Sharifi, M., Hasan, A., Attar, F., Edis, Z., Bai, Q., Derakhshankhah, H., Falahati, M., 2021c. Magnetic nanocatalysts as multifunctional platforms in cancer therapy through the synthesis of anticancer drugs and facilitated Fenton reaction. J. Adv. Res. 30, 171.

Khan, S., Vahdani, Y., Hussain, A., Haghighat, S., Heidari, F., Nouri, M., Bloukh, S.H., Edis, Z., Babadaei, M.M.N., Ale-Ebrahim, M., 2021d. Polymeric micelles functionalized with cell penetrating peptides as potential pH-sensitive platforms in drug delivery for cancer therapy: A review. Arabian J. Chem., 103264

Li, S., Shang, L., Xu, B., Wang, S., Gu, K., Wu, Q., Sun, Y., Zhang, Q., Yang, H., Zhang, F., 2019. A nanozyme with photo-enhanced dual enzyme-like activities for deep pancreatic cancer therapy. Angew. Chem. 131, 12754–12761.

Liu, J., Liu, K., Zhang, L., Zhong, M., Hong, T., Zhang, R., Gao, Y., Li, R., Xu, T., Xu, Z.P., 2021a. Heat/pH-boosted release of 5-fluorouracil and albumin-bound paclitaxel from Cu-doped layered double hydroxide nanomedicine for synergistical chemo-phototherapy of breast cancer. J. Control. Release 335, 49–58.

Liu, Q., Zhang, A., Wang, R., Zhang, Q., Cui, D., 2021b. A review on metal-and metal oxide-based nanozymes: Properties, mechanisms, and applications. Nano-micro Lett. 13, 1–53.

Ma, L., Chen, X., Li, J., Chang, H., Schwank, J.W., 2020. Electronic metal-support interactions in Pt/FeOx nanospheres for CO oxidation. Catal. Today 355, 539–546.

Ma, Z., Wu, L., Han, K., Han, H., 2019. Pt nanozyme for O_2 self-sufficient, tumor-specific oxidative damage and drug resistance reversal. Nanoscale Horiz. 4, 1124–1131.

Moutabian, H., Majdaeen, M., Ghahramani-Asl, R., Yadollahi, M., Gharepapagh, E., Ataei, G., Falahatpour, Z., Bagheri, H., Farhood, B., 2022. A systematic review of the therapeutic effects of resveratrol in combination with 5-fluorouracil during colorectal cancer treatment: with a special focus on the oxidant, apoptotic, and anti-inflammatory activities. Cancer Cell Int. 22, 1–14.

Noguchi, S., Takagi, A., Tanaka, T., Takahashi, Y., Pan, X., Kibayashi, Y., Mizokami, R., Nishimura, T., Tomi, M., 2021. Fluorouracil uptake in triple-negative breast cancer cells: Negligible contribution of equilibrative nucleoside transporters 1 and 2. Biopharm. Drug Dispos. 42, 85–93.

Poller, J.M., Zaloga, J., Schreiber, E., Unterweger, H., Janko, C., Radon, P., Eberbeck, D., Trahms, L., Alexiou, C., Friedrich, R.P., 2017. Selection of potential iron oxide nanoparticles for breast cancer treatment based on in vitro cytotoxicity and cellular uptake. Int. J. Nanomed. 12, 3207.

Pooresmaeil, M., Asl, E.A., Namazi, H., 2021a. A new pH-sensitive CS/Zn-MOF@ GO ternary hybrid compound as a biofriendly and implantable platform for prolonged 5-Fluorouracil delivery to human breast cancer cells. J. Alloys Compd. 885, 160992.

Pooresmaeil, M., Asl, E.A., Namazi, H., 2021b. A new pH-sensitive CS/Zn-MOF@GO ternary hybrid compound as a biofriendly and implantable platform for prolonged 5-Fluorouracil delivery to human breast cancer cells. J. Alloys Compd. 885, 160992.

Prylutska, S., Grynyuk, I., Skaterna, T., Horak, I., Grebinyk, A., Drobot, L., Matyshevska, O., Senenko, A., Prylutskyy, Y., Naumovets, A., 2019. Toxicity of C60 fullerene–cisplatin nanocomplex against Lewis lung carcinoma cells. Arch. Toxicol. 93, 1213–1226.

Prylutska, S., Lynchak, O., Kostjukov, V., Evstigneev, M., Remeniak, O., 2019b. Antitumor effects and hematotoxicity of C60-Cis-Pt nanocomplex in mice with Lewis lung carcinoma.

Rashid, R.A., Abidin, S.Z., Anuar, M.A.K., Tominaga, T., Akasaka, H., Sasaki, R., Kie, K., Razak, K.A., Pham, B.T., Hawkett, B.S., 2019. Radiosensitization effects and ROS generation by high Z metallic nanoparticles on human colon carcinoma cell (HCT116) irradiated under 150 MeV proton beam. OpenNano 4, 100027.

Rottenberg, S., Disler, C., Perego, P., 2021. The rediscovery of platinum-based cancer therapy. Nat. Rev. Cancer 21, 37–50.

Sápi, A., Kéri, A., Kálomista, I., Dobó, D.G., Ákos, S., Juhász, K.L., Ákos, K., Kónya, Z., Galbács, G., 2017. Determination of the platinum concentration of a Pt/silica nanocomposite decorated with ultra small Pt nanoparticles using single particle inductively coupled plasma mass spectrometry. J. Anal. At. Spectrom. 32, 996–1003.

Semenza, G.L., 2016. The hypoxic tumor microenvironment: A driving force for breast cancer progression. Biochimica et Biophysica Acta (BBA) – Mol. Cell Res. 1863, 382–391.

Sharifi, M., Bai, Q., Babadaei, M.M.N., Chowdhury, F., Hassan, M., Taghizadeh, A., Derakhshankhah, H., Khan, S., Hasan, A.,

Falahati, M., 2021. 3D bioprinting of engineered breast cancer constructs for personalized and targeted cancer therapy. J. Control. Release 333, 91–106.

Sharifi, M., Faryabi, K., Talaei, A.J., Shekha, M.S., Ale-Ebrahim, M., Salihi, A., Nanakali, N.M.Q., Aziz, F.M., Rasti, B., Hasan, A., Falahati, M., 2020a. Antioxidant properties of gold nanozyme: A review. J. Mol. Liq. 297, 112004.

Sharifi, M., Hasan, A., Nanakali, N.M.Q., Salihi, A., Qadir, F.A., Muhammad, H.A., Shekha, M.S., Aziz, F.M., Amen, K.M., Najafi, F., Yousefi-Manesh, H., Falahati, M., 2020b. Combined chemo-magnetic field-photothermal breast cancer therapy based on porous magnetite nanospheres. Sci. Rep. 10, 5925.

Sharifi, M., Hosseinali, S.H., Yousefvand, P., Salihi, A., Shekha, M.S., Aziz, F.M., JouyaTalaei, A., Hasan, A., Falahati, M., 2020c. Gold nanozyme: biosensing and therapeutic activities. Mater. Sci. Eng., C 108, 110422.

Sharifi, M., Jafari, S., Hasan, A., Paray, B.A., Gong, G., Zheng, Y., Falahati, M., 2020d. Antimetastatic Activity of Lactoferrin-Coated Mesoporous Maghemite Nanoparticles in Breast Cancer Enabled by Combination Therapy. ACS Biomater. Sci. Eng. 6, 3574–3584.

Sharifi, M., Rezayat, S.M., Akhtari, K., Hasan, A., Falahati, M., 2020e. Fabrication and evaluation of anti-cancer efficacy of lactoferrin-coated maghemite and magnetite nanoparticles. J. Biomol. Struct. Dyn. 38, 2945–2954.

Shueng, P.-W., Yu, L.-Y., Chiu, H.-C., Chang, H.-C., Chiu, Y.-L., Kuo, T.-Y., Yen, Y.-W., Lo, C.-L., 2021. Early phago-/endosomal escape of platinum drugs via ROS-responsive micelles for dual cancer chemo/immunotherapy. Biomaterials 276, 121012.

Skivka, L.M., Prylutska, S.V., Rudyk, M.P., Khranovska, N.M., Opeida, I.V., Hurmach, V.V., Prylutskyy, Y.I., Sukhodub, L.F., Ritter, U., 2018. C60 fullerene and its nanocomplexes with anticancer drugs modulate circulating phagocyte functions and dramatically increase ROS generation in transformed monocytes. Cancer Nanotechnol. 9, 1–22.

Song, L., Huang, C., Zhang, W., Ma, M., Chen, Z., Gu, N., Zhang, Y., 2016 Oct. Graphene oxide-based Fe2O3 hybrid enzyme mimetic with enhanced peroxidase and catalase-like activities. Colloids and Surfaces A: Physicochemical and Engineering Aspects. 5 (506), 747–755.

Tang, Q., Liu, D., Chen, H., He, D., Pan, W., Li, Q., Xie, W., Chen, S., Yu, C., 2022. Functionalized PAMAM-Based system for targeted delivery of miR-205 and 5-fluorouracil in breast cancer. J. Drug Delivery Sci. Technol. 67, 102959.

Tsai, T.-L., Lai, Y.-H., Chen, H.H., Su, W.-C., 2021. Overcoming Radiation Resistance by Iron-Platinum Metal Alloy Nanoparticles in Human Copper Transport 1-Overexpressing Cancer Cells via Mitochondrial Disturbance. Int. J. Nanomed. 16, 2071.

Watanabe, T., Oba, T., Tanimoto, K., Shibata, T., Kamijo, S., Ito, K.-I., 2021. Tamoxifen resistance alters sensitivity to 5-fluorouracil in a subset of estrogen receptor-positive breast cancer. PLoS ONE 16, e0252822.

Xiao, Y., Huang, G., Xiang, Y., 2021. Research on Anti-Tumor Nano-Particle with New Type 5-Fluorouracil on the Peritoneal Metastasis of Breast Cancer. J. Biomater. Tissue Eng. 11, 1277–1283.

Xu, L., Wang, J., 2012. Magnetic Nanoscaled /Ce Composite as an Efficient Fenton-Like Heterogeneous Catalyst for Degradation of 4-Chlorophenol. Environ. Sci. Technol. 46, 10145–10153.

Yang, Z., Sun, N., Cheng, R., Zhao, C., Liu, Z., Li, X., Liu, J., Tian, Z., 2017. pH multistage responsive micellar system with charge-switch and PEG layer detachment for co-delivery of paclitaxel and curcumin to synergistically eliminate breast cancer stem cells. Biomaterials 147, 53–67.

You, Q., Zhang, K., Liu, J., Liu, C., Wang, H., Wang, M., Ye, S., Gao, H., Lv, L., Wang, C., 2020. Persistent Regulation of Tumor Hypoxia Microenvironment via a Bioinspired Pt-Based Oxygen Nanogenerator for Multimodal Imaging-Guided Synergistic Phototherapy. Adv. Sci. 7, 1903341.

Zhao, H., Wang, D., Gao, C., Liu, H., Han, L., Yin, Y., 2016. Ultrafine platinum/iron oxide nanoconjugates confined in silica nanoshells for highly durable catalytic oxidation. J. Mater. Chem. A 4, 1366–1372.

Zhao, N., Yan, L., Xue, J., Zhang, K., Xu, F.-J., 2021. Degradable one-dimensional dextran-iron oxide nanohybrids for MRI-guided synergistic gene/photothermal/magnetolytic therapy. Nano Today 38, 101118.

Zheng, M., Mei, Z., Junaid, M., Tania, M., Fu, J., Chen, H.-C., Khan, M.A., 2022. Synergistic Role of Thymoquinone on Anticancer Activity of 5-Fluorouracil in Triple Negative Breast Cancer Cells. Anti-Cancer Agents Med. Chem. (Formerly Curr. Med. Chem.-Anti-Cancer Agents) 22, 1111–1118.

Zorrilla-Veloz, R.I., Stelzer, T., López-Mejías, V., 2018. Measurement and correlation of the solubility of 5-fluorouracil in pure and binary solvents. J. Chem. Eng. Data 63, 3809–3817.

Zou, T., Lu, W., Mezhuev, Y., Lan, M., Li, L., Liu, F., Cai, T., Wu, X., Cai, Y., 2021. A review of nanoparticle drug delivery systems responsive to endogenous breast cancer microenvironment. Eur. J. Pharm. Biopharm. 166, 30–43.